International Research Journal of Engineering and Technology (IRJET) e-ISSN: 2395-0056
Volume: 09 Issue: 12 | Dec 2022 www.irjet.net p-ISSN: 2395-0072

Soil moisture estimation using Land Surface Temperature in the Northwestern coast of Egypt

Noha M. Youssef[1], Ashraf M. El Moustafa[2], Mohamed A. Gad[3], Dina M. Elleithy[4]

[1] Ph.D. student, Faculty of Engineering, Ain shams university, Civil engineer, Water Resources Research Institute, National Water Research Center, Ministry of Water Resources and Irrigation, Egypt
[2,3] Professor of Engineering Hydrology, Irrigation and Hydraulics Department, faculty of engineering, Ain shams university, Egypt
[4] Assistant professor, Irrigation and Hydraulics Department, faculty of engineering, Ain shams university, Egypt

---

Abstract - *Soil moisture is one of the main hydro-meteorological variables that play an important role in processes related to infiltration and runoff generation. Nowadays remote sensing techniques can detect surface soil moisture, compensating for the shortage of in-situ measuring techniques. This work aims to test the capability of thermal bands of Landsat-8 datasets in detecting surface soil moisture in a semi-arid environment and to investigate the temporal variation of soil moisture during three different time slots (2016, 2021, and 2022) representing different soil moisture conditions. The low rates of soil moisture content (SMC) in November 2021 represent the dry season due to the absence of rainfall, and the high SMC in January 2016 and February 2022 represents the rainy season due to the antecedent rainfall. Also, the sensitivity of the observed and predicted soil moisture content to the antecedent rainfall storms was discussed. Band 10 was used to determine the land surface temperature (LST) and convert it to soil moisture index (SMI). Measurements of (SMC) were carried out at several locations in the mainstream of Agarma watershed, a tributary of wadi Kharouba, Matrouh, Northwest of Egypt as a representation of a semi-arid environment. A linear regression analysis was selected to generate a relationship between the observed (SMC) and the estimated (SMI) for the three dates, also the validation of soil moisture was considered. The validation results showed that the coefficient of determination (R^2) between SMC and SMI for three days in (2016, 2021, and 2022) were 0.83, 0.80, and 0.89 respectively.*

Keywords: Soil moisture, Soil moisture index, Land surface temperature, Landsat-8

1. Introduction

Soil moisture is essential in the global water cycle and other aspects of earth science [1] and is a crucial variable for hydrology, meteorology, and agriculture [2]. It is a key element in understanding the hydrological process as it regulates the infiltration-runoff mechanism. Hence, researchers are keen to estimate precise soil moisture for a variety of applications, including flood and drought prediction in hydrology [3]. In-situ measurements and remote sensing technology are examples of soil moisture monitoring technologies. For small-scale applications, in-situ measurements of soil moisture are accurate [4], whereas estimates of soil moisture obtained from remote sensing using various techniques (optical, thermal infrared, and microwave) are suitable for large-scale applications in a few upper centimeters of soil [5]. The majority of regions worldwide suffer from a lack of soil moisture measurements, therefore remote sensing compensates such lack by providing soil moisture data with varying spatial and temporal resolutions all over the world [6]. Different studies [8, 9] noted that the emitted and reflected radiations are sensitive to soil moisture conditions. Accurate retrieved soil moisture is enhancing the estimation of runoff and groundwater recharge [6, 7]. Landsat-8 thermal bands are effective for identifying the existence of shallow water by estimating land surface temperature (LST) [10]. Many authors [11, 12, 13] established various approaches for measuring soil moisture content (SMC) based on soil reflectance and LST. Soil moisture index (SMI) proposed by [14] is a relationship between LST and normalized difference vegetation index (NDVI). SMI values vary from 0 for dry conditions to 1 for moist conditions. [15] developed SMI by utilizing another relationship between maximum and minimum land surface temperature (LST).

Recently, [10] estimated the soil moisture index (SMI) using thermal remote sensing to define waterlogged areas in Ismailia governorate, Egypt based on land surface temperature computation. Datasets of Landsat 5, 7, and 8 were used to estimate LST, and SMI during three different dates (1998, 2008, and 2015). Validation of soil moisture was carried out only in 2015 and obtained a moderate correlation R^2 equal to 0.61. The results showed that the

Spatio-temporal variations of soil moisture were related to Land-use/Land-cover and water table levels.

While [16] used Landsat-7 and Sentinel-1 data to investigate the change in soil moisture content for one measurement only in August 2016 regarding crop patterns in the east of the Nile Delta of Egypt. Two methodologies were utilized based on LST and backscattering coefficient determination. Two correlations were generated between observed soil moisture content and the estimated SMI & backscattering coefficient. Results showed good R^2 = 0.81 and 0.83 for both types of datasets (Landsat-7 and Sentinel-1) respectively. Also, results ensured that the discrimination of crop types was related to the distribution of soil moisture.

On the other hand, [17] applied another methodology to estimate SMI using sentinel-2 data in wadi Kharouba, Northwest of Egypt. Shortwave Transformed Reflectance STR and Normalized Difference Vegetation Index NDVI were calculated and an optical trapezoidal model (OPTRAM) was established to obtain SMI. R^2 was generated between the observed soil moisture and the estimated SMI at different depths from 10 cm to 30 cm in Jan. 2016 only. Results ensured that correlation of observed soil moisture and estimated SMI at 10 cm was better than their values at 20 and 30 cm.

The current work aims to generate a correlation between the observed soil moisture content (SMC), and the estimated soil moisture index (SMI) from the thermal bands of Landsat-8 and investigates the temporal variation of soil moisture related to different rainfall intensities during different periods in the rainy season of a semi-arid environment (Northwestern coast of Egypt).

2. Materials and methods

The Northwestern coast of Egypt is characterized by a high rate of rainfall in the rainy season from September to April. Rainfed farming is the primary source of food for the majority of the local Bedouins on Egypt's Northwestern Coast and acts as one of the major economical pillars for them. As per [18] "Egypt's coastal zone must be developed because it has the most promising land for agricultural expansion". The region has a lot of wadis filled with natural vegetation, rain-fed crops, and olive and fig trees in the mainstream, where wadi deposits are located [19]. The classification of the soil type of the Northwestern coast of Egypt (from Fuka to Matrouh) was shallow sandy soil and deep sandy loam to loam soil [20], and was characterized by sandy clay loam and sandy loam texture described in El-Hraka Basin [21]. Most of the land cover in the main wadis of the Northwestern coast of Egypt was classified to rainfed crops and bare soil. For example, Wadi El Raml had three main types of land cover such as rainfed crops, sparsely vegetated land, and bare soil [19]. Also, the same classification was founded in El-Hraka Basin as per [21].

2.1 Study area description

Wadi Kharouba, located in Matrouh governorate, Northwestern coast of Egypt, is having an area of 38 km^2. It lies between latitudes 31° 11' 0''N, 31° 22' 0''N, and longitudes 27° 10' 30''E and 27° 20' 0''E. It is bordered from the North by Matrouh city and from the west by wadi El Raml. The climate of the region is characterized by a short rainy winter and long hot dry in summer, whereas the average annual temperature is about 24.5°C in Matrouh [21] and the average annual rainfall varies between 100 mm and 190 mm [22]. Figure (1) shows the Agarma watershed, a tributary of wadi Kharouba with an area of 6 km^2, which was chosen to conduct several soil moisture content measurements. Figure (2a) shows the land cover of wadi Kharouba created by using the Landsat-8 bands and the supervised classification technique and was classified into three categories rainfed crops, sparse grass, and bare soil. While figure (2b) shows the ASTER Global Digital Elevation Model (GDEM) of wadi Kharouba, where the low elevations represent the rainfed crop areas and the high elevations represent the sparse grass area and bare soil. On the other side, soil samples were collected from Agarma watershed and analyzed in the laboratory. The results indicated a sandy clay loam texture that was matching the description of the soil texture of the same watershed mentioned in [22].

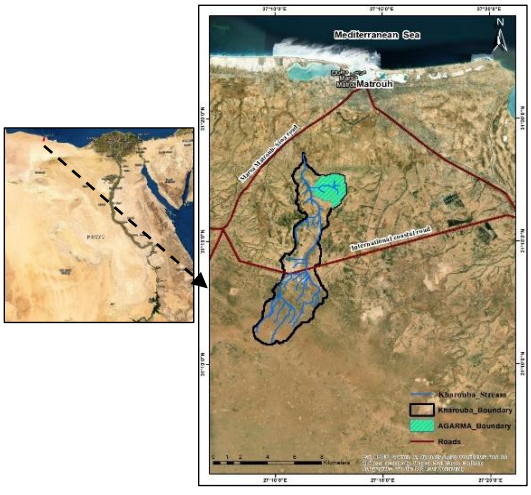

Figure 1: Location map of Wadi Kharouba

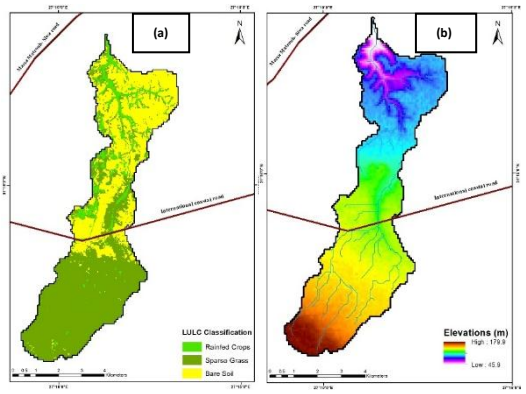

Figure 2: a) Land cover classes **b)** digital elevation model (DEM) of wadi Kharouba

2.2 Data sets

2.2.1 In-situ soil moisture measurements

Soil moisture measurements were taken at twenty locations along the mainstream of Agarma watershed, figure (3). Theta Probe soil moisture sensor type ML2X was used with a measuring depth of 5 to 10 cm. Measuring started consequently from the downstream (point 1) in a curved line, following the mainstream path, till (point 20) at the most upstream. Runoff concentration in the mainstream, low elevations, and agricultural activities made these locations more promising for the estimation of soil moisture. These locations were studied before in the MARSADEV project carried out by the Mediterranean Agronomic Institute of Bari and provided this current work by only one measurement on 16 January 2016 at the twenty locations [17, 22].

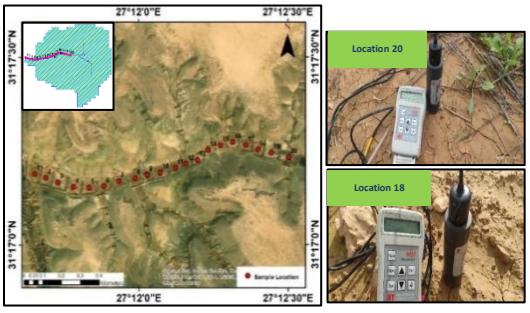

Figure 3: Location of soil moisture measurements in Agarma watershed

One historical record of soil moisture in Agarma watershed was available in the literature on 16 Jan.2016 [17]. In addition, new measurements were performed on 10 Nov.2021 and 6 Feb.2022. Figure (4) shows the observed soil moisture measurements at the twenty locations in Agarma watershed for those dates. High values were observed in Feb 2022 and moderate were recorded in Jan.2016, while the other low values were measured in Nov 2021.

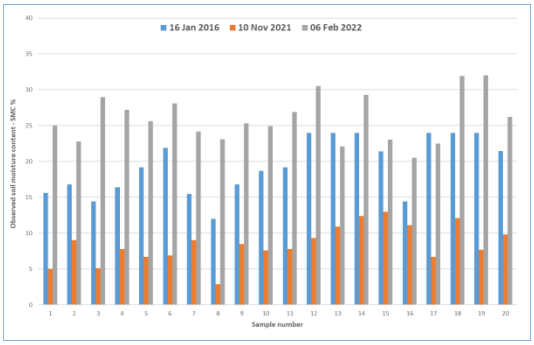

Figure 4: Observed soil moisture content (SMC%) for different dates in Agarma watershed

Landsat-8 data were downloaded close to the dates of field measurements and according to their availability. Table (1) shows the details of both measured and acquired data, in addition to the recorded rainfall information in Matrouh before and after the measurement dates.

Table 1: Details of measured and acquired data

Measuring Date	Available Acquisition Date Landsat-8 (OLI/TIRS)	Rainfall status during the measuring and acquisition dates in (mm) Source: Water Resources Research Institute. WRRI
16-Jan-2016	21-Jan-2016	12.2 mm on 31-Dec-2015 No rainfall from 1 Jan. to 21 Jan.2016
10-Nov-2021	2-Nov-2021	No rainfall over the study area from the start of the rainy season in September till 20 Nov.2021
6-Feb-2022	6-Feb-2022	12.2 mm on 2-Jan-2022 15.5 mm on 13-Jan-2022 11.2 mm on 26-Jan-2022 No rainfall from 27-Jan-to 6 Feb.2022

All acquired scenes mentioned above in table (1) contain low cloud cover and are far from the study area, hence they were used in the analysis after processing. While another acquired scene with the corresponding field measurement in Dec.2021, was not considered in the analysis due to the dense cloud cover over the study area. Table (1) also shows that there was a time gap between measuring time and acquisition time in 2016 and 2021 due

to the revisit time of Landsat every 16 days. Therefore, it was deemed necessary to report the rainfall events recorded during such a period, as it is one of the variables that will affect the soil moisture content.

2.2.2 Remote sensing data used

The Landsat-8 data with two sensors (Operational Land Imager OLI/Thermal Infrared Sensor TIRS) were used and downloaded from USGS [27] website https://earthexplorer.usgs.gov/. Downloading was carried out by defining the location of the study area using (Path/Row:179/38), and the data were acquired in the three target periods. Table (2) describes the specifications of Landsat-8 (OLI/TIRS) data.

Table 2: Specifications of Landsat-8 (OLI/TIRS) data

Specifications	Landsat-8 (OLI/TIRS)
Spatial Resolution	30 m (OLI) except Panchromatic band B8=15 m 30 m (TIRS)
Temporal Resolution	16 days
Product Level	Collection 1&2 Level-1
Detection depth	0 – 7.5 cm

2.3 Land Surface Temperature (LST) computation

Computation of LST required doing a lot of corrections on the thermal bands of Landsat-8 (B10&B11), figure 5. The thermal atmospheric correction was applied using ENVI software to remove the atmospheric contribution from thermal infrared radiance data. While radiometric calibration was used by calibrating the corrected thermal bands to radiance, reflectance, or brightness temperatures. On the other hand, land Surface Emissivity LSE (Ɛ) is one of the key parameters for retrieving accurate LST from remotely sensed imagery [23]. The resulting top of atmospheric spectral radiance (TOA), at-sensor brightness temperature, and emissivity were included in the land surface temperature LST calculation using the algorithm [24]. Three atmospheric functions (ψ_1, ψ_2, ψ_3) were involved in LST calculation based on equation (1) and defined from the seasonal-latitude surface temperature model available in ENVI 5.3.

$$T_s = \gamma \left(\varepsilon_{10} \left(\psi_1 * L_{10\ sensor} + \psi_2\right) + \psi_3\right) + \delta^{-1} \quad (1)$$

Where: T_s is LST in (Kelvin), ε_{10}: is emissivity for band 10, and the L_{10} sensor is Band 10 radiance.

$$\gamma \approx T^2_{10\ sensor} / (b\ \gamma . L_{10\ sensor}) \quad (2)$$

$$\delta \approx T_{10\ sensor} - (T^2_{10\ sensor} / b\ \gamma) \quad (3)$$

Where: $T_{10sensor}$ is Band 10 at-sensor brightness temperature, λ_{10}: Band 10 effective wavelength, b $\gamma = c_2/\lambda =$ (1324 K) and (ψ_1, ψ_2, ψ_3) are atmospheric functions.

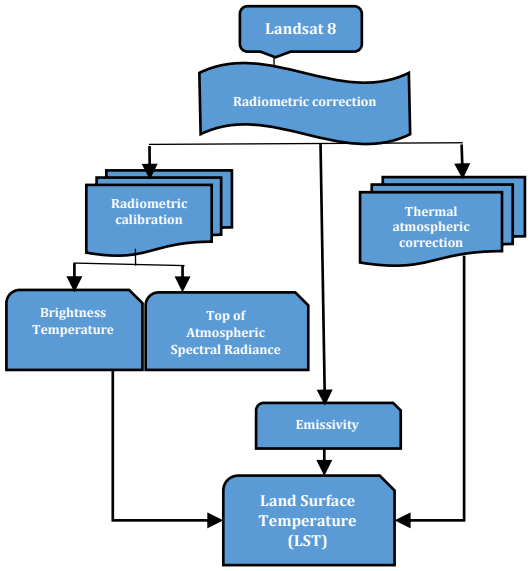

Figure 5: Flow chart of Land Surface Temperature (LST) computation

2.3.1 Soil Moisture Index estimation (SMI)

The soil moisture index (SMI) is the ratio of the difference between present soil moisture and the permanent wilting point to field capacity and residual soil moisture. This indicator ranges from 0 to 1, with 0 representing dry conditions and 1 representing moist conditions [25]. Determination of SMI requires the computation of the maximum and minimum values of LST [15] as explained in equation (4).

$$SMI = (LST_{max} - LST) / (LST_{max} - LST_{min}) \quad (4)$$

Where: SMI is Soil Moisture Index, LST_{max}, LST_{min}, and LST: are the maximum, minimum, and value of the retrieved LST respectively.

By applying the previously mentioned methodology of land surface temperature (LST) estimation and using equation 4 for computing the soil moisture index (SMI), LST and SMI maps of Kharouba watershed were created for the three measuring days of Jan. 2016, Nov.2021, and Feb.2022, figure (6) and figure (7) respectively.

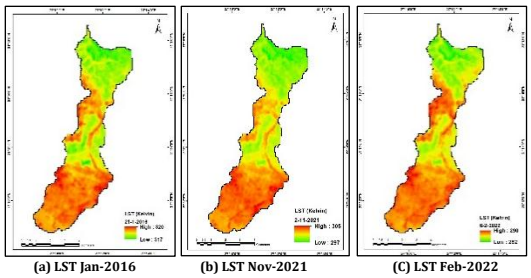

Figure 6: Land surface temperature (LST) maps of Kharouba watershed

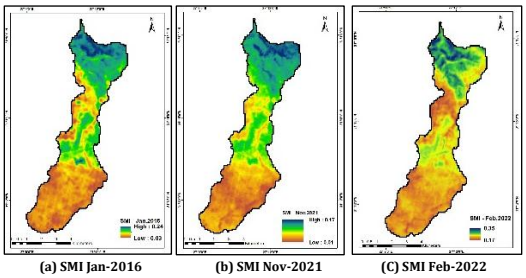

Figure 7: Retrieved Soil moisture indices (SMIs) of Kharouba watershed

Figures 6 and 7 show the variation in soil moisture indices that were related to LST changes, where high temperatures were accompanied by low soil moisture content and vice versa. The lowest values of the estimated SMI were observed in Nov.2021, while the highest values were estimated in Feb.2022. And the values of retrieved SMI in Jan.2016 had moderate values.

In addition, the variation in soil moisture was correlated with the types of land cover mentioned before in wadi Kharouba, where rainfed crops corresponded to an increase in SMI, while the bare soil and areas covered by grass have low values of SMI.

3. Validation of soil moisture content using Landsat-8 data

A linear regression analysis was created between the measured soil moisture content SMC of 20 samples in Agarma watershed and the estimated SMI for different dates (Jan.2016, Nov.2021, and Feb.2022). 14 readings for each of those dates were utilized to calibrate the model between SMC and SMI. Six readings were selected randomly for validation as shown in figure 8.

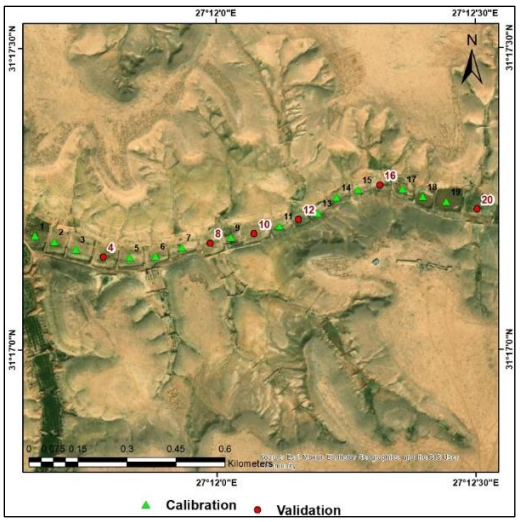

Figure 8: Selected samples for calibration and validation

The coefficient of determination (R^2), equation (5), was used to evaluate the generated model between observed SMC and estimated SMI.

$$R^2 = \left[\frac{\sum_{i=1}^{N}(Y_i-\bar{Y})(X_i-\bar{X})}{\sqrt{\sum_{i=1}^{N}(Y_i-\bar{Y})^2}\sqrt{\sum_{i=1}^{N}(X_i-\bar{X})^2}}\right]^2 \quad (5)$$

Where Yi and Xi are the observed (SMC) and estimated (SMI) respectively, $\bar{Y}$ and $\bar{X}$ are their mean values respectively, and N is the total number of observations.

Other statistical measures such as Root Mean Square Error (RMSE), Equation (6), and Mean Absolute Error (MAE), Equation (7), were calculated to assess the validation of soil moisture.

$$RMSE = \sqrt{\frac{1}{N}\sum_{i=1}^{N}(Y_i - X_i)^2} \quad (6)$$

Where Y_i and X_i are the observed and estimated soil moisture respectively, and N is the total number of data.

$$MAE = \frac{1}{N}\sum_{i=1}^{N} abs(Y_i - X_i) \quad (7)$$

Where Y_i and X_i are the observed and estimated soil moisture respectively, and N is the total number of data.

RMSE measures the difference between satellite estimates (SMI) and observed data (SMC), it has a range from 0 to ∞; values close to zero reflect the high accuracy of satellite estimates in contrast to high values [26].

While Mean Absolute Error (MAE) indicates the ratio between the sum of absolute errors to the total number of data. The lower values of MAE are representing the higher accuracy of satellite data [26].

The generated relations between SMC and SMI for the historical measurement on 16 Jan.2016 beside the other new measurements on 10 Nov.2021 and 6 Feb.2022 are described below. Also, the results of the validation assessment are presented as follows:

Measurements from Literature (January 2016)

Both values of observed SMC and estimated SMI in this event had medium values compared with values in November 2021 and February 2022, as a result of 12.2 mm of rainfall storm occurred on 31 December 2015 over the study area,16 days before ground measurements of SMC. Equation (8) and figure (9) show the relation between the observed soil moisture content and the retrieved soil moisture index in Jan.2016 with the resulting $R^2 = 0.72$.

$$SMI = 0.6244\ SMC + 0.0371 \quad (8)$$

Where SMI is the estimated soil moisture index from Landsat-8 and SMC is the observed soil moisture content.

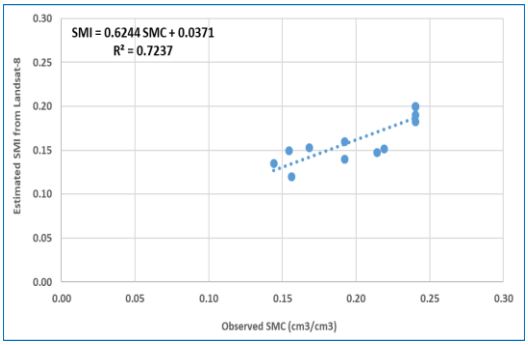

Figure 9: Linear regression analysis between observed soil moisture SMC and estimated SMI (Jan-2016)

Figure (10a) shows the results of soil moisture validation in January 2016 with a good R^2 equal to 0.83 and the values of RMSE and MAE are 0.03 and 0.02 respectively. Also, the map of spatial variations of the predicted soil moisture of wadi kharouba is presented in figure (10b), where predicting the soil moisture was estimated based on the proposed model shown in equation 8 using a raster calculator.

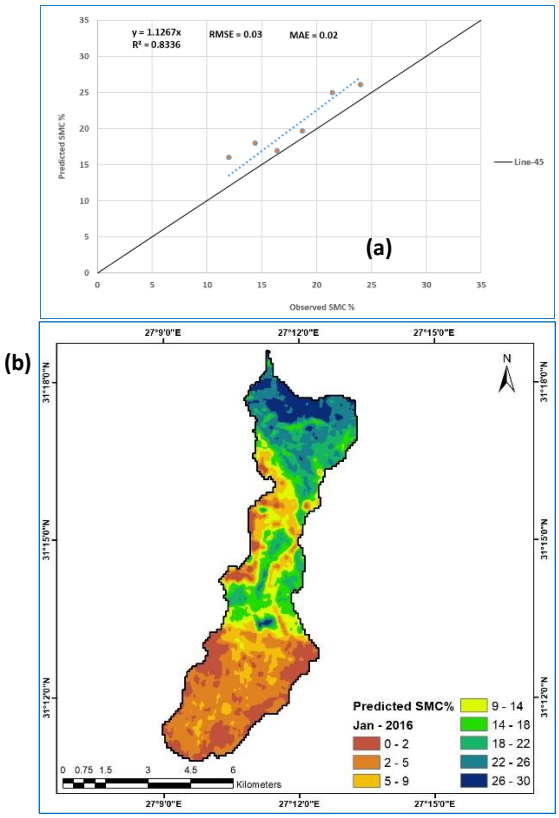

Figure 10: a) Assessment of soil moisture validation **b)** Predicted soil moisture content SMC % (Jan-2016)

Measurements in (November 2021)

Due to the absence of rainfall before the measurements on 10 November 2021, as per table 1, values of the observed soil moisture content in this event were the lowest. Figure (11) and equation (9) show the generated model between the observed SMC and estimated SMI in Nov.2021. The resulting coefficient of determination (R^2) was equal to 0.66.

$$SMI = 0.399\ SMC + 0.0914 \quad (9)$$

Where SMI is the estimated soil moisture index from Landsat-8 and SMC is the observed soil moisture content.

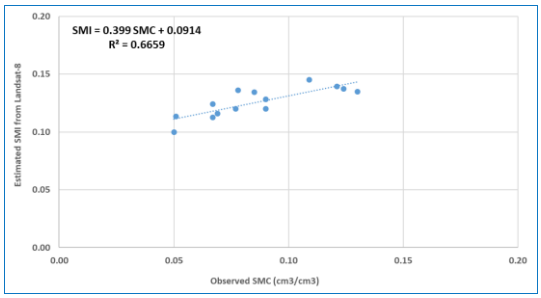

Figure 11: Linear regression analysis between observed soil moisture SMC and estimated SMI (Nov-2021)

The resulting R^2 from validation and the values of RMSE and MAE were 0.80, 0.01, and 0.01 respectively as shown in figure (12a). While the predicted SMC % was created in Nov. 2021 over wadi Kharouba, figure (12b) using the previously generated model (equation 9). Almost the whole watershed was covered with very low values of soil moisture content except the small cultivated areas in the North and that represents the dry season.

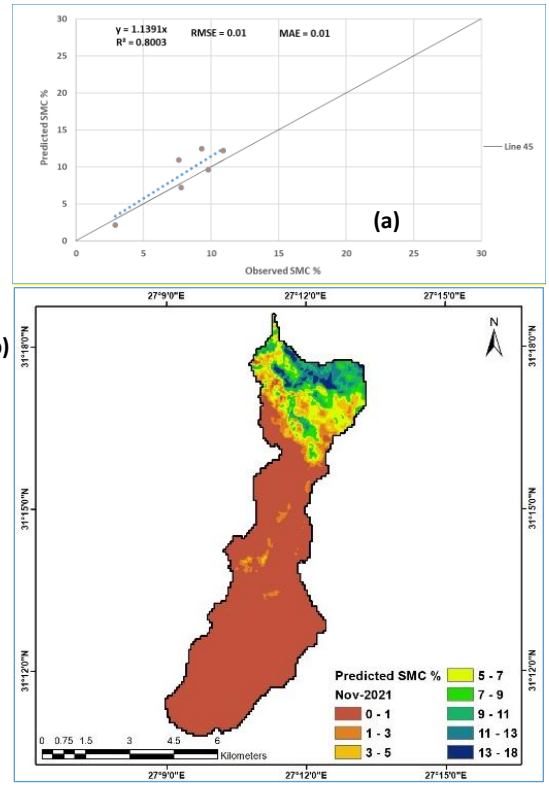

Figure 12: a) Assessment of soil moisture validation **b)** Predicted soil moisture content SMC % (Nov-2021)

Measurements in (February 2022)

The highest soil moisture values were recorded in February 2022 due to three rainfall events of a total depth of 39 mm that occurred in three days on 2, 13, and 26 January 2022 covering the study area. Figure (13) and equation (10) show the result of linear regression analysis between the observed SMC and estimated SMI in Feb.2022 including the value of resulted R^2 was equal to 0.69.

$$SMI = 0.2181\ SMC + 0.2619 \qquad (10)$$

Where SMI is the estimated soil moisture index from Landsat-8 and SMC is the observed soil moisture content.

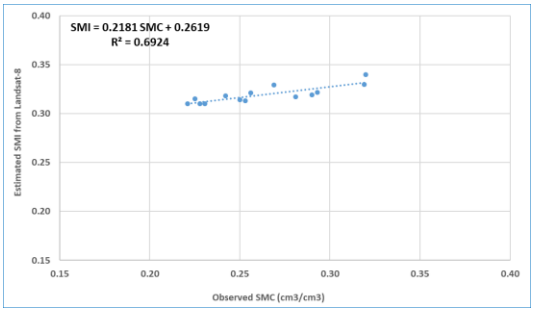

Figure 13: Linear regression analysis between observed soil moisture SMC and estimated SMI (Feb-2022)

The results of the validation are shown below in figure (14a), whereas the best R^2 calculated for Feb-2022 readings was equal to 0.89 and the values of RMSE and MAE were 0.019 and 0.017 respectively. On the other hand, the values of predicted SMC % ranged from 0 to 40 %, figure (14b), and these values were extreme from all predictions due to the antecedent rainfall storms before measuring.

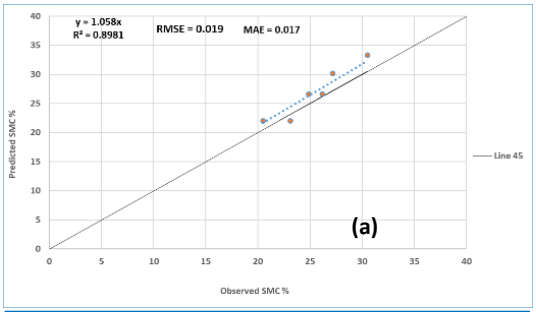

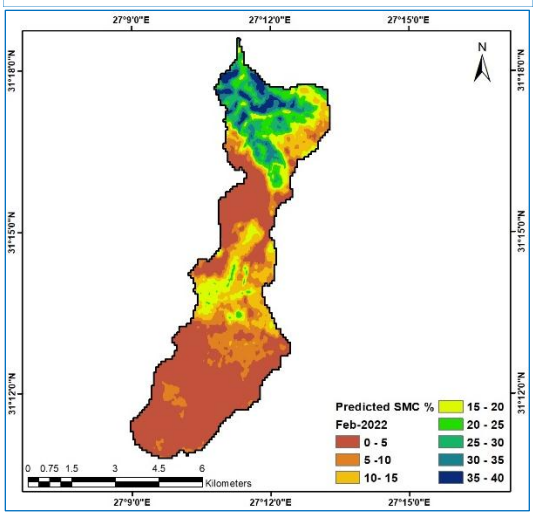

Figure 14: a) Assessment of soil moisture validation **b)** Predicted soil moisture content SMC % (Feb-2022)

From the previous analysis and results, it can be concluded that the soil moisture values were very sensitive to the intensity of rainfall and the duration of the dry period before the measurement date. Also, the results of the validation showed good indicators such as R^2 that varied from 0.80 to 0.89, RMSE ranged from 0.01 to 0.03, and the MAE differed from 0.01 to 0.02. Moreover, 18 readings from all measurements were validated and both observed and predicted soil moisture are presented in figure (15). The figure shows that the differences between the observed and predicted soil moisture range from 0.01 to 0.04 and it can be considered very small.

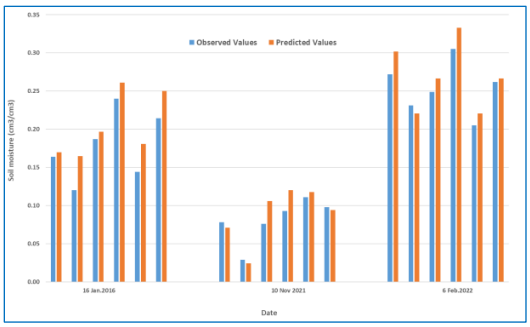

Figure 15: Observed and predicted values of soil moisture content

4. Summary and Conclusion

Landsat-8 OLI/TIRS data were utilized to assess the Spatio-temporal distribution of the soil moisture content during three days (Jan.2016, Nov.2021, and Feb.2022) at 20 different locations in Agarma watershed on the Northwestern coast of Egypt. One historical record of soil moisture content in 2016 was considered in the analysis, and new measurements were executed in November 2021 and February 2022 using the Theta Probe soil moisture sensor type ML2X with 5 to 10 cm measuring depth. The soil type of selected locations was defined from the laboratory texture analysis as sandy clay loam. While the land cover of the study area was classified as rainfed crops, sparse grass, and bare soil respectively. A correction procedure was applied to obtain both the land surface temperature (LST) and the soil moisture index (SMI) from Landsat-8 band-10. The methodology included different corrections processing for band-10 such as the thermal atmospheric and radiometric corrections. The maps of LST and SMI were created for the three different dates. In addition, a linear regression analysis was performed between the observed soil moisture and estimated SMI for each date of ground measurements. Also, the validation was carried out to evaluate the generated relations between observed and predicted soil moisture. The best coefficient of determination R^2 was equal to 0.89 for the data sets in February 2022 because there was no gap between the measuring and acquisition dates of these datasets. In addition, the generated three relations between observed soil moisture content and estimated soil moisture index were correlated with the intensity of rainfall, whereas the values of soil moisture in November 2021 were the lowest as a result of rainfall absences. And the highest values were in January 2016 and February 2022 due to the antecedent rainfall storms. Therefore, it was concluded that the obtained relation between SMC and SMI using the data of November 2021 could be used

for estimating SMC in the dry season. While the first and the third generated relations represent the rainy season. Lastly, the values of predicted soil moisture content were very close to the observed ones, and the methodology of obtaining the land surface temperature and soil moisture index using the thermal bands of Landsat-8 is recommended to map the soil moisture over a large scale.

5. Acknowledgment

This research was supported by the Science and Technology Development Fund (STDF) through the research project “Strategies for increasing the WATER use efficiency of semi-arid Mediterranean Watersheds and agrosilvopastoral systems under climate Change (SWATCH)” which was awarded through a PRIMA call. The PRIMA program is an Art.185 initiative supported and funded under Horizon 2020, the European Union's Framework Program for European Commission.

6. References

[1] Carsten pathe, wolfgang wagner, Daniel sable, marcela doubkova, and Jeffrey b.basara, "Using ENVISAT ASAR Global mode data for surface soil moisture retrieval over Oklahoma, USA," IEEE transactions on geoscience and remote sensing, vol.47, No.2, 2009, PP.468-479.

[2] Ansari, S., Deshmukh, R. R," Estimation of Soil Moisture Content: A Review", International Journal of Theoretical and Applied Mechanics, vol.12, No.3, 2017, PP.571–577.

[3] Walker, J.P., Houser, P.R," A methodology for initializing soil moisture in a global climate model: assimilation of near-surface soil moisture observations". Journal of Geophysical Research–Atmospheres, vol.106, No.11, 2001, PP.11761–11774.

[4] Chen, Y.; Yang, K.; Qin, J.; Cui, Q.; Lu, H.; La, Z.; Han, M.; Tang, W, "Evaluation of SMAP, SMOS, and AMSR2 soil moisture retrievals against observations from two networks on the Tibetan Plateau". J. Geophysics. Res. Atoms, vol.122, 2017, PP.5780–5792.

[5] Rötzer, K.; Montzka, C.; Bogena, H.; Wagner, W.; Kerr, Y.H.; Kidd, R.; Vereecken, H, "Catchment scale validation of SMOS and ASCAT soil moisture products using hydrological modeling and temporal stability analysis". J. Hydrol., vol.519, 2014, PP.934–946.

[6] C. Alvarez-Garreton, D. Ryu, A. W. Western, W. Crow, D. Robertson, "Impact of observation error structure on satellite soil moisture assimilation into a rainfall-runoff model", 20th International Congress on Modelling and Simulation, 2013, Adelaide, Australia.

[7] Lihua Xiong and Ling Zeng, "Impacts of Introducing Remote Sensing Soil Moisture in Calibrating a Distributed Hydrological Model for Streamflow Simulation", Water, vol.11, 2019, PP.1-20.

[8] D. Chen, Engman, E.T. and Brutsaert, W, ”Spatial distribution and pattern persistence of surface soil moisture and temperature over prairie from remote sensing", Remote Sensing of Environment, vol.61, 1997, PP. 347-360.

[9] Dubayah, R., Wood, E.F. and Lavallee, D, "Multi-scaling analysis in distributed modeling and remote sensing: an application using soil moisture. In Quartrochhi, D., and Goodchild, M. (Eds.), Scale in remote sensing and GIS", New York, NY: Lewis, 1996, PP. 93-112.

[10] A.M. Hassan, A.A. Belal, M.A. Hassan, F.M. Farag, E.S. Mohamed, "Potential of thermal remote sensing techniques in monitoring waterlogged area based on surface soil moisture retrieval", Journal of African Earth Sciences, vol.155, 2019, PP. 64–74.

[11] Wang, L., Qu, J.J., Hao, X, "Forest fire detection using the normalized multiband drought index (NMDI) with satellite measurements", Agric. Forest Meteorology, vol.148, No.11, 2008, PP. 1767–1776.

[12] Haas, J, "Soil moisture modelling using TWI and satellite imagery in the Stockholm region". M.Sc. dissertation, School of Architecture and the Built Environment, Royal Institute of Technology (KTH), 2010, Stockholm, Sweden, TRITAGIT EX 10-001.

[13] El-Zeiny, A.M., Effat, H.A, "Environmental monitoring of spatiotemporal change in land use/land cover and its impact on land surface temperature in El-Fayoum governorate. Egypt". Remote Sensing Applications: Society and Environment, vol.8, 2017, PP.266–277.

[14] Zeng, Y., Feng, Z., Xiang, N, "Assessment of soil moisture using Landsat ETM + Temperature /

vegetation index in semiarid environment". IEEE, 2004, PP. 4306–4309.

[15] Moawad, B.M, "Geoscience general tool package". Max-Planck Institute fürChemie, 2012, Mainz, Germany.

[16] E.S. Mohamed, Abdelraouf Ali, Mohammed El-Shirbeny, Khaled Abutaleb, Sameh M. Shaddad, "Mapping soil moisture and their correlation with crop pattern using remotely sensed data in arid region", The Egyptian Journal of Remote Sensing and Space Sciences, vol.23, 2020, PP. 347–353.

[17] Abdelmaqsoud Mostafa, "Retrieving soil moisture content by using satellite data: a case study of Wadi Kharouba, Egypt", MSc thesis, 2021, Mediterranean Agronomic Institute of Bari, Bari, Italy.

[18] Negm, A.M. and Abu-Hashim, M, "Sustainability of Agricultural Environment in Egypt: Part II", 2019, Soil-Water- Plant Nexus.

[19] Ashraf N. El-Sadek and Ahmed H. Mohamed, "Simulation of the Effect of Land Cover Change on Water Balance and Sediment Yield of Wadi El Raml in the Northwestern Coast, Egypt", Alexandria science exchange journal, vol.38, No.4, 2017.

[20] El-Nahry A and Rashash A, "Rain Water Harvesting Using GIS and RS for Agriculture Development in Northwestern Coast, Egypt", Journal of Geography & Natural Disasters, vol.5, No. 2, 2015.

[21] El Husieny A. Abou Hussien, M. Ismail, Wail M. Omran, and Mohamed S. Abou Alfotoh, "Water Harvesting for Sustainable Development of El-Hraka Basin in The Northwestern Coast of Egypt", Egypt. J. Soil. Sci. Vol. 60, No. 3, 2020, PP. 263- 276.

[22] Mohamed Ahmed Ibrahim Abdallah, "A rainfall-runoff model for water management in wadi systems based on hydropedological studies, MSC thesis, 2017, Mediterranean Agronomic Institute IAMB, Bari, Italy.

[23] Sobrino, J.A.; Raissouni, N.; Li, Z, "A comparative study of land surface emissivity retrieval from NOAA data". Remote Sens. Environ, vol.75, 2001, PP. 256–266.

[24] Jimenez-Munoz, J.C., Sobrino, J.A, "A generalized single-channel method for retrieving land surface temperature from remote sensing data", J. Geophysics. Res. Vol.108, 2003, https://doi.org/10.1029/2003JD003480.

[25] Chandrasekar, K, "Geospatial Meteorological Products for Agricultural Drought Assessment", NRSC User Interaction Meet-PPT, 2016.

[26] Willmott, C. J., Ackleson, S. G., Davis, R. E., Feddema, J. J., Klink, K. M., Legates, D. R., O'Donnell, J., and Rowe, C. M, "Statistics for the evaluation and comparison of models". Journal of Geophysical Research, vol.90, No.C5, 1985, PP.8995, https://doi.org/10.1029/jc090ic05p08995.

[27] US Geological Survey (USGS), "Landsat 8 (L8) Science Data Users Handbook", vol. 2, 2016, PP. 60–61.